PERFORMANCE ANALYSIS OF A NOVEL SIX-STROKE OTTO CYCLE ENGINE

by

Emre ARABACI*

Department of Automotive Technology, Vocational School of Technical Science,
Burdur Mehmet Akif Ersoy University, Burdur, Turkey

Original scientific paper
https://doi.org/10.2298/TSCI190926144A

In this study, a simulation model with finite time thermodynamics was presented for an Otto cycle six-stroke engine. In this six-stroke engine, two free strokes occur after the exhaust stroke. These free strokes cause the engine to have higher thermal efficiency. Due to high thermal efficiency, these six-stroke engines can be used in hybrid electric vehicles. In this study, the effect of residual gas fraction and stroke ratio on the effective power and effective thermal efficiency were investigated. In addition, heat balance was obtained for the engine and the use of fuel energy in the engine was examined with the help of performance fractions. In the simulation model, the results are quite realistic as the working fluid was assumed to consist of fuel-air-residual gases mixture.

Key words: *engine performance, thermodynamic model, Otto cycle, six-stroke engine, engine simulation*

Introduction

It is possible to see that internal combustion engines are used everywhere. Since the invention of internal combustion engines, it has been subjected to many innovative changes [1, 2]. These changes take place within the triangle consisting of performance, economy and environment [3]. Today, Otto and Diesel cycle engines are widely used. These engines are engineered by many engine researchers and designers for both fuel economy, high power and low exhaust emissions [4-6]. Atkinson and Miller cycle engines are also being designed, in particular by modifying the heat rejection processes of conventional heat cycles to increase thermal efficiency [7-9]. It is desirable for the range-extender engines in hybrid-electric vehicles to have high thermal efficiency. In the same way, the engines used in electric generators operate at constant speed and these engines are required to have high thermal efficiency [10]. There are also five-stroke engines that guarantee high thermal efficiency [11].

As an alternative to conventional internal combustion engines, there are also six-stroke engines. Despite the fact that these engines were first designed in the 1880's, they are still expected to be developed and used as a potential nowadays. It is basically a modified version of the four-stroke engines and is usually high thermal efficiency focused designs [12-15]. Six-stroke engines can be described as engines that allow two additional strokes to occur in the conventional four-stroke engine cycle after exhaust stroke [16, 17]. Generally, exhaust heat recovery methods are used to increase thermal efficiency in six-stroke engines [18, 19].

* Author's e-mail: earabaci@mehmetakif.edu.tr

There are also six-stroke engine designs in which the free-stroke method is used instead of the exhaust heat recovery method. The main purpose of these designs is to change the initial conditions of the cycle. The idea of the six-stroke engine design with free-stroke method was first proposed by Kelem and Kelem [20]. Their main purpose in this design is to clean and cool the cylinder with air thanks to free strokes. Thus, it is aimed to increase the volumetric efficiency and thermal efficiency. The exhaust valve or a third valve remain open during the free strokes. Here, the first free stroke is the second intake stroke, the second free stroke is the second exhaust stroke. Since the same valve remains open in these sequential strokes, the flow direction in the manifold is changing. However, the design of the valve mechanism, which allows the exhaust valve to remain open for a long time, appears to be quite simple and practical. In this study, this design of Kelem and Kelem [20] was slightly modified. In the free strokes after the exhaust stroke, instead of the continuous exhaust valve (or third valve) being open, the intake and exhaust valves are opened in the first and second free stroke, respectively, fig. 1. In the first free stroke (free intake) only the intake valve is open and fresh air-flows into the cylinder. In the second free stroke (free exhaust) only the exhaust valve is open and the working fluid in the cylinder is ejected. In this way, the exhaust manifold flow problems in their design are largely eliminated. In fig. 1, it is seen that the novel six-stroke engine consists of conventional four strokes and two free strokes. The four-stroke engine completes one cycle in two crank revolutions, while the six-stroke engine completes one cycle in three crank revolutions.

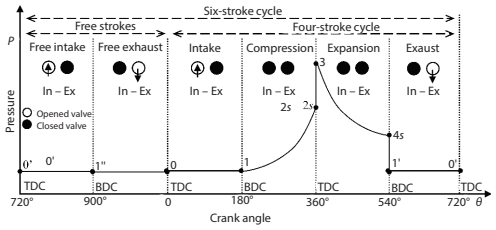

Figure 1. Pressure crank angle diagram for six-stroke Otto engine cycle

Atkinson or Miller cycle engines are preferred today due to their high thermal efficiency especially for hybrid electric vehicles. As the expansion ratio is greater than the compression ratio, such engines are also called over-expanded (or extended expansion) engines. Interestingly, although the engines used in these vehicles have high thermal efficiency, the power/volume ratio is low compared to conventional engines. Over-expanded engines are also modified as conventional engines, such as six-stroke engines, and both engines offer high thermal efficiency. The cycle is fully extended instead of the expansion process on six-stroke engines. This results in fewer cycles for the same engine speed.

It can be assumed that the theoretical thermodynamic cycle takes place in a finite time so that the relationship between the thermodynamic cycles of the theoretical heat engines and the actual engine cycles can be explained more realistically. This method is called the finite time thermodynamics method. However, in these models, theoretical cycle models can be brought closer to the actual cycles by taking into account the actual cycle losses. Since it is both practical and suitable for parametric studies, the finite time thermodynamics method is frequently preferred for quasi-realistic or realistic models of actual internal combustion engines [21, 22]. Thanks to the finite time thermodynamics method, the effects of many design parameters on engine performance can be examined. There are many studies in the literature examining the effects of design parameters on engine performance [23-33]. With the finite time thermodynamics method, the effects of many design parameters such as stroke length [23, 24], stroke/bore ratio [25], friction loss [26], compression ratio [27], residual gas fraction [28], and combustion efficiency [29] on engine performance can be examined in detail. In theoretical cycles in classical thermodynamics, the working fluid is considered to be air. In the finite time thermodynamics method, the working fluid can be defined only as air [30, 31] or air-fuel mixture [32] or air-fu-

el-residual gas mixture [33]. As can be seen, finite time thermodynamics method can be widely used in modelling of actual engines according to theoretical cycles.-

There are no studies in the literature that examined the performance of six-stroke engines. However, the six-stroke engine concept examined in this study was modeled by simulating a conventional four-stroke engine. In this study, the effects of design parameters on engine performance, irreversibility, friction, heat transfer losses were also taken into consideration.

Simulation model

The thermodynamic model of the both cycles are similar because the six-stroke engines are the modified versions of the four-stroke engines. The pressure-volume, *Pv*, and temperature-entropy, *Ts*, diagrams for cycles are illustrated in fig. 2. The presented model is used to simulate both cycle processes and to examine the effects of design parameters on engine performance. Thanks to this model, the effects of design parameters on engine performance can be examined and design properties for optimum performance are determined. Subscript, s, is used for cases where the compression and expansion processes are reversible and the processes are indicated by dashed line. The sequential numbering in fig. 2 is made according to fig. 1. When the *Pv* diagram is examined, points 0 → 1 → 2 → 3 → 4 → 1′ → 0 represent irreversible four-stroke Otto cycle engine and points 0 → 1 → 2 → 3 → 4 → 1′ → 0′ →1″ →0 represent irreversible six-stroke Otto cycle engine. Here 0′ →1″ and 1″ → 0 processes are free-intake and free-exhaust strokes for the six-stroke cycle engine. With these two processes, the in-cylinder temperature and the residual gas fraction are relatively reduced. It is modeled assuming that both engine cycles occur at points 1 → 2 → 3 → 4 → 1. However, the characteristics of the point 1 are different from each other in both engine cycles. The main reason for this is that in six-stroke engines, the temperature and residual gas fraction at the point 1 is lower than four-stroke engines due to the two free strokes that occur after the exhaust stroke [12-14].

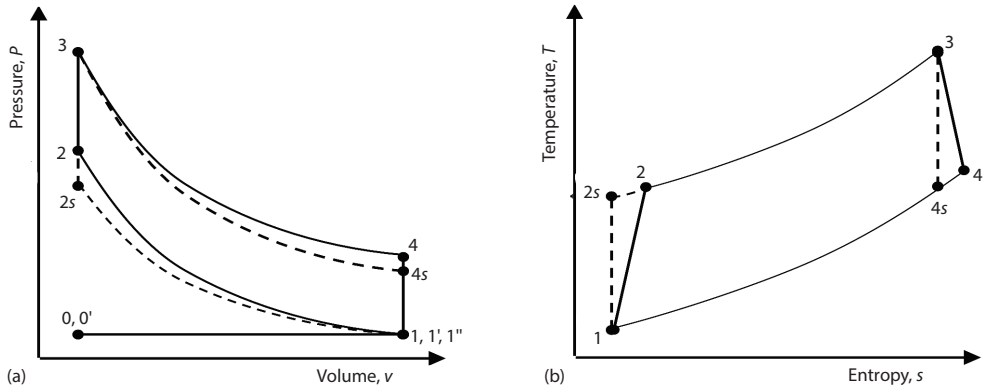

Figure 2. Diagrams for Otto cycle; (a) pressure-volume and (b) temperature-entropy [28, 30, 34]

The simulation flowchart is shown in fig. 3. In this simulation, engine performance can be optimized for maximum effective power or maximum effective thermal efficiency using input parameters.

It is assumed that the working fluid, $\dot{m}_{\text{mix}}$, is a mixture of air, $\dot{m}_a$, fuel, $\dot{m}_f$, and residual gases, $\dot{m}_r$, and that the fuel mass per second, $\dot{m}_f$, for both cycles is constant [28, 33]:

$$\dot{m}_{\text{mix}} = \dot{m}_a + \dot{m}_f + \dot{m}_r = \dot{m}_f \frac{\left(\phi + x_{AFs}\right)}{\phi\left(1 - x_r\right)} \tag{1}$$

where ϕ, x_{AFs}, and x_r are equivalence ratio, stoichiometric air/fuel ratio, and residual gas fraction, respectively, x_r – the expressed as $\dot{m}_r/\dot{m}_{\text{mix}}$. For the six-stroke engine, $\dot{m}_{\text{mix6}}$ is expressed as follows. Subscript 6 is used to refer to a six-stroke engine:

$$\dot{m}_{\text{mix}6} = \dot{m}_{a6} + \dot{m}_{f6} + \dot{m}_{r6} = \dot{m}_f \frac{\left(\phi + x_{AFs}\right)}{\phi\left(1 - x_{r6}\right)} \tag{2}$$

where $\dot{m}_{f6} = \dot{m}_f$, it is $\dot{m}_{a6} = \dot{m}_a$ but $\dot{m}_{r6} < \dot{m}_r$ and $x_{r6} < x_r$. In the free intake process in the six-stroke engine, only the air-flows into the cylinder, and the in-cylinder concentration of the residual gases decreases depending on the compression ratio, ε. In the free exhaust process, the air-residual gases mixture in the cylinder is discharged and the residual gas fraction is relatively reduced. At the end of the exhaust and free exhaust processes, it is assumed that the residual gas fraction is the same. Since the exhaust gas is actually composed of a mixture of residual gas and air at the end of the free exhaust stroke, x_{r6} was used to express the actual residual gas fraction in the cylinder. Thus, the relationship between x_r and x_{r6} is defined:

$$x_{r6} = \frac{x_r}{\varepsilon + 1} \tag{3}$$

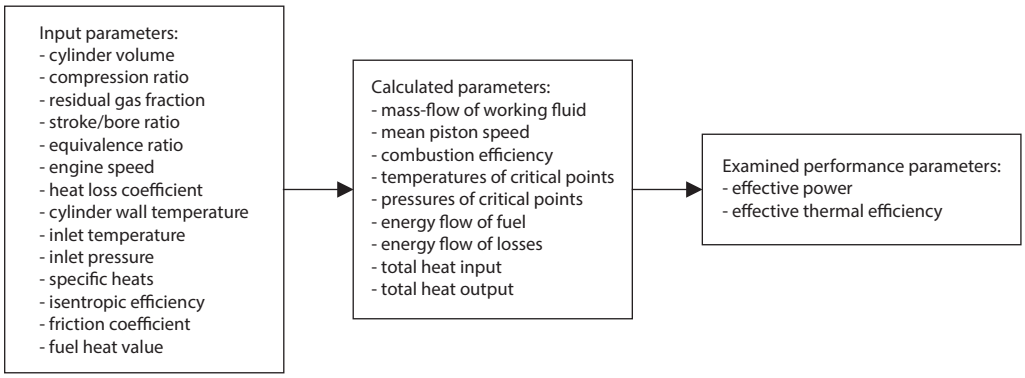

Figure 3. Simulation flow chart of the four- and six-stroke Otto cycle engine

Accordingly, in this simulation model, x_r is used for four-stroke engines and x_{r6} – the used for six-stroke engines. This is the same for all the next equations. The specific heats for the working fluid are considered to be constant. However, since the working fluid is composed of the air-fuel-residual gas mixture, specific temperatures vary depending on ϕ and x_r. Accordingly, the constant volume specific heat, $c_{v\text{mix}}$, and the gas constant, R_{mix}, for the working fluid are formulated [28]:

$$c_{v\text{mix}} = \frac{\left(1 - x_r\right)\left(x_{AFs}c_{va} + \phi c_{vf}\right) + x_r\left(\phi + x_{AFs}\right)c_{vr}}{\phi + x_{AFs}} \tag{4}$$

$$R_{\text{mix}} = \frac{\left(1 - x_r\right)\left(x_{AFs}R_a + \phi R_f\right) + x_r\left(\phi + x_{AFs}\right)R_r}{\phi + x_{AFs}} \tag{5}$$

The end of the compression process temperature, T_{2s}, and the end of the expansion process temperature, T_{4s}, are formulated [22, 28, 34]:

$$T_{2s} = \exp\left[\frac{R_{\text{mix}} \ln(\varepsilon) + c_{v\text{mix}} \ln(T_1)}{c_{v\text{mix}}}\right] \tag{6}$$

$$T_{4s} = \exp\left[\frac{-R_{\text{mix}} \ln(\varepsilon) + c_{v\text{mix}} \ln(T_3)}{c_{v\text{mix}}}\right] \tag{7}$$

However, it was accepted that there was irreversibility in these processes in the model. Therefore, T_2 and T_4 should be determined instead of T_{2s} and T_{4s}. In order to express these irreversibility, the compression process isentropic efficiency, η, and the expansion process isentropic efficiency, η_e, is used. Thus, T_2 and T_4 can be calculated [22, 34]:

$$T_2 = \frac{T_{2s} - T_1}{\eta_c} + T_1 \tag{8}$$

$$T_4 = \left(T_{4s} - T_3\right)_{\ e} + T_3 \tag{9}$$

The total heat input per second, Q_{in}, and total heat output per second, Q_{out}, are in constant volume in the Otto cycle [28, 34]:

$$\dot{Q}_{\text{in}} = \dot{m}_{\text{mix}} c_{v\text{mix}} \left(T_3 - T_2\right) = \frac{\dot{m}_f}{\phi}\left[\left(x_{AF\text{s}} c_{va} + \phi c_{vf}\right) + x_r c_{vr}\right]\left(T_3 - T_2\right) \tag{10}$$

$$\dot{Q}_{\text{out}} = \dot{m}_{\text{mix}} c_{v\text{mix}} \left(T_4 - T_1\right) = \frac{\dot{m}_f}{\phi}\left[\left(x_{AF\text{s}} c_{va} + \phi c_{vf}\right) + x_r c_{vr}\right]\left(T_4 - T_1\right) \tag{11}$$

where $\dot{Q}_{\text{in}}$ is also equal to the difference in fuel energy flow, $\dot{Q}_f$, and heat transfer loss, $\dot{Q}_{ht}$, during the combustion process [33, 35]:

$$\dot{Q}_{\text{in}} = \dot{Q}_f - \dot{Q}_{ht} \tag{12}$$

$\dot{Q}_f$ and $\dot{Q}_{ht}$ are expressed [27, 29, 31]:

$$\dot{Q}_f = \eta_{com} \dot{m}_f H_u = \left(-1.4474 + \frac{4.1858}{\phi} - \frac{1.86876}{\phi^2}\right) \dot{m}_f H_u \tag{13}$$

$$\dot{Q}_{\text{ht}} = \dot{m}_{\text{mix}} \beta\left(T_2 + T_3 - 2T_w\right) = \dot{m}_f \frac{\left(\phi + x_{AF\text{s}}\right)}{\phi\left(1 - x_r\right)} \beta\left(T_2 + T_3 - 2T_w\right) \tag{14}$$

where η_{com}, H_u, and β are the combustion efficiency, lower heat value of fuel, total heat loss coefficient, respectively, η_{com} is defined as a function of ϕ, H_u and β were accepted as constant [28].

The effective power, P_e, and effective thermal efficiency, η_{th}, are defined as the performance parameters [36]:

$$P_{\text{e}} = \dot{Q}_{\text{in}} - \dot{Q}_{\text{out}} - P_\mu \tag{15}$$

$$\eta_{th} = \frac{P_{\text{e}}}{\dot{Q}_f} \tag{16}$$

where P_μ is the friction loss power and is the function of the friction coefficient, μ, and the average piston speed, c_m, [36]. Here, the same equation is used for both engine cycles. Although the cycle is 50% longer (which means more friction loss) in six-stroke engines, 50% less cycles occur for the same piston speed:

$$P_\mu = \mu\left(c_m\right)^2 = \frac{\mu N^2}{900}\left[\frac{4\lambda^2 \dot{m}_{\text{mix}} R_{\text{mix}} T_1\left(\varepsilon - 1\right)}{P_1 \pi \varepsilon}\right]^{2/3} \tag{17}$$

where λ is the ratio of stroke length to cylinder diameter [34]:

$$\lambda = \frac{L}{D} = \frac{4v_d}{\pi D^3} = \frac{4v_t\left(\varepsilon - 1\right)}{\pi \varepsilon D^3} \tag{18}$$

where T_1 is generally considered to be equal to T_0, which is the reference temperature. However, the air-fuel mixture taken into the cylinder at the temperature T_0 – the mixed with the residual gas at temperature T_4. The T_1 is therefore, expressed as a function of T_0, T_4, R_r, and R_{mix} [33, 34]:

$$T_1 = \frac{T_0\left(\dot{m}_a R_a + \dot{m}_f R_f\right) + \dot{m}_r R_r T_4}{\dot{m}_{\text{mix}} R_{\text{mix}}} = T_0 + \frac{x_r R_r\left(T_4 - T_0\right)}{R_{\text{mix}}} \tag{19}$$

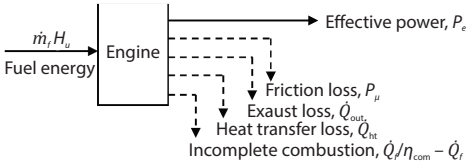

Figure 4. Typical heat balance for internal combustion engines

Only a part of the fuel energy flow is converted by the engine into the effective power. The power lost that cannot be converted into effective power is caused by friction, exhaust, heat transfer and incomplete combustion, fig. 4. This power lost is also called performance lost.

The ratio of performance lost to fuel energy is expressed as the performance lost fraction. The performance lost fractions resulting from exhaust, F_{ex}, friction, F_μ, heat transfer, F_{ht}, and incomplete combustion, F_{inc}, are expressed [35]:

$$F_{\text{ex}} = \frac{\dot{Q}_{\text{out}}}{\dot{m}_f H_u} = \frac{\dot{Q}_{\text{out}}}{\frac{\dot{Q}_f}{\eta_{com}}} \tag{20}$$

$$F_\mu = \frac{P_\mu}{\dot{m}_f H_u} = \frac{P_\mu}{\frac{\dot{Q}_f}{\eta_{com}}} \tag{21}$$

$$F_{\text{ht}} = \frac{\dot{Q}_{\text{ht}}}{\dot{m}_f H_u} = \frac{\dot{Q}_{\text{ht}}}{\frac{\dot{Q}_f}{\eta_{com}}} \tag{22}$$

$$F_{\text{inc}} = \frac{\dot{Q}_f}{\dot{m}_f H_u} = \left(1 - \eta_{com}\right) \tag{23}$$

The performance fraction can be defined:

$$F_{pe} = \frac{\dot{m}_f H_u - \left(F_{\text{ex}} + F_\mu + F_{\text{ht}} + F_{\text{inc}}\right)}{\dot{m}_f H_u} = \frac{P_{\text{e}}}{\dot{m}_f H_u} = \frac{P_{\text{e}}}{\frac{\dot{Q}_f}{\eta_{com}}} = \eta_{th}\eta_{com} \tag{24}$$

All variables can be calculated by equations 1-24 when specific heats (c_{va}, c_{vf}, c_{vr}), gas constants (R_a, R_f, R_r), x_r, λ, ϕ, ε, v_t, x_{AFs}, N, P_1, T_0, T_w, β, η_c, η_e, and μ are known. For the six-stroke engine x_{r6} is used instead of x_r for calculations.

Numerical study and discussion

In this comprehensive study, the effect of x_r and λ on the performance of both the four- and the six-stroke Otto cycle engine has been investigated in detail with the simulation model developed. As a result of this numerical study, design criteria for a six-stroke engine were examined in detail and remarkable data were obtained, tab. 1.

Table 1. Design parameters for numerical study [22-36]

Parameter	Value	Unit
Total cylinder volume, v_t	500	[cm^3]
Engine speed, N	4000	[rpm]
Isentropic efficiencies, η_c and η_e	0.97	
Stoichiometric air-fuel ratio, xAF_s	15.05 (for gasoline)	
Reference temperature, T_0	300	[K]
Cylinder wall temperature, T_w	400	K
Reference pressure, $P_0 = P_1$	100	[kPa]
Heat loss coefficient, β	0.5	[kJkg^{-1}K^{-1}]
Friction coefficient, μ	12.9	[Nsm^{-1}]
Lower heat value	44790 (for gasoline)	[kJkg^{-1}]
Specific heats, (c_{va}/ c_{vf}/c_{vr})	0.718/1.638/0.866	[kJkg^{-1}K^{-1}]
Gas constants, (R_a/R_f/R_r)	0.287/0.07/0.307	[kJkg^{-1}K^{-1}]
Equivalence ratio, ϕ	1.00	
Stroke ratio, λ	0.5 → 1.5	
Residual gas fraction, x_r	0.05 → 0.25	
Compression ratio, ε	2 → 100	

Figure 5 shows the change in critical point temperatures depending on the compression ratio. When T_1 is examined, it is seen that the six-stroke engine has a lower initial cycle temperature than the four-stroke engine. This is actually a parameter that increases the volumetric efficiency. The value of T_1 varies depending on ε, T_4, and x_r, eq. (19). For the case where x_r is fixed, x_{r6} to ε for the six-stroke engine is inversely proportional, eq. (3). In addition, T_4 for the six-stroke engine is slightly higher than the four-stroke engine. It is seen that T_4 and ε are inversely proportional. The main reason for the low T_1 in the six-stroke engine is that x_{r6} is very low compared to x_r. As T_1 is low in the six-stroke engine, T_2 is also low. The higher x_r, the lower the maximum combustion temperature. As the x_{r6} is lower than the x_r, the maximum cycle temperature T_3 is slightly higher in the six-stroke engine.

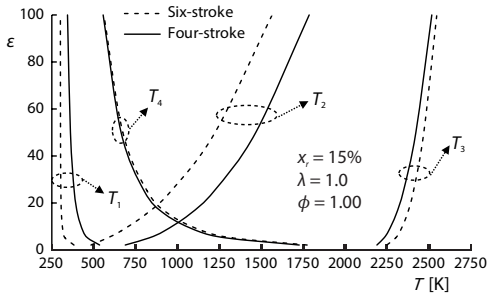

Figure 5. Variations of compression ratio, ε, temperatures of critical points, T, at fixed residual gas fraction, x_r, stroke ratio, λ, and equivalence ratio, ϕ

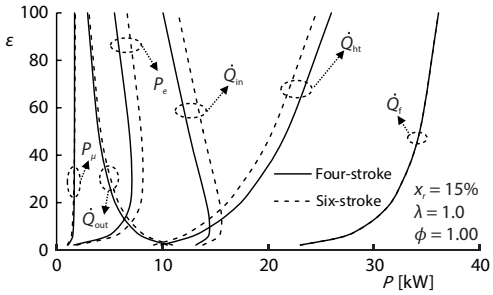

Figure 6. Variations of compression ratio, ε, powers (or heat flows), P, at fixed residual gas fraction, x_r, stroke ratio, λ, and equivalence ratio, ϕ

Figure 6 illustrates the variation of $\dot{Q}_{\text{in}}$, $\dot{Q}_{\text{out}}$, $\dot{Q}_{\text{ht}}$, $\dot{Q}_f$, P_e, and P_μ depending on ε. In the simulation model, $\dot{Q}_f$ trend is the same for both engines because it is assumed that $\dot{m}_f$ and $\dot{m}_{f6}$ are equal in order to compare the performance of the four- and the six-stroke engine. However, $\dot{Q}_f$ increases as the $\dot{m}_f$ increases with the increase of ε for fixed v_t. The $\dot{Q}_{\text{ht}}$ varies depending on T_2 and T_3 and is proportional to ε. The $\dot{Q}_{\text{in}}$, which is equal to the difference between $\dot{Q}_f$ and $\dot{Q}_{\text{ht}}$, increases first and then decreases depending on ε. The $\dot{Q}_{\text{out}}$ depends on the difference between T_4 and T_1. Because the T_4 and T_1 difference are higher in the six-stroke engine than the four-stroke engine, $\dot{Q}_{\text{out}}$ is slightly higher in the six-stroke engine. The P_μ varies according to μ and c_m, eq. (17). According to the simulation model, although $\dot{m}_f = \dot{m}_{f6}$, due to the x_r, and x_{r6} relationship in the simulation model, $\dot{m}_{\text{mix}} \neq \dot{m}_{\text{mix6}}$. For both engines, P_μ is almost equal. Depending on ε, P_e increases first and then decreases.

Figure 7 demonstrates the effect of ε on η_{th} for the case where x_r, λ , and ϕ are constant. As ε increases, η_{th} increases first and then decreases. It also shows that the expression *thermal efficiency increases as the compression ratio is increased* in classic thermodynamics does not apply when using a realistic thermodynamic model as here. Because when the losses such as friction, heat transfer and irreversibilities are taken into account, the change in the thermal efficiency depending on the compression ratio is as follows. It is clearly seen here that the six-stroke engine has higher thermal efficiency than the four-stroke engine.

Figure 8 shows the effect of λ on P_e, and η_{th} when x_r and ϕ are fixed. For high speed engines, $\lambda > 1$. When λ increases, P_μ increases, so P_e decreases. When it is desired to have high P_e and η_{th}, $\lambda > 1$ should be required.

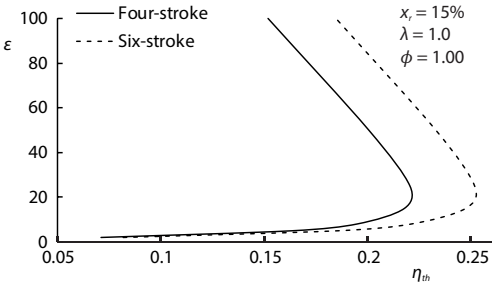

Figure 7. Variations of compression ratio, ε, effective thermal efficiency, η_{th}, at fixed residual gas fraction, x_r, stroke ratio, λ, and equivalence ratio, ϕ

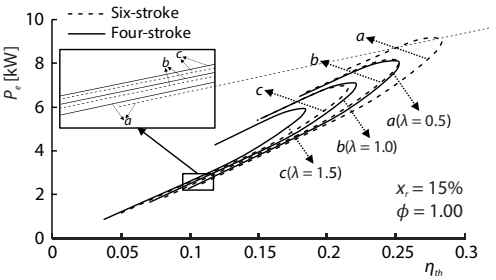

Figure 8. Variations of effective power, P_e, effective thermal efficiency, η_e, against to stroke ratio, λ, at fixed residual gas fraction, x_r, and equivalence ratio, ϕ

In fig. 9, as x_r decreases, the maximum value of η_{th} for the four-stroke engine increases significantly, while that of the six-stroke engine is almost unchanged. As x_r increases, $\dot{m}_f$ decreases and therefore, $\dot{Q}_f$ decreases. When x_r increases P_e decreases significantly. The advantage of this six-stroke engine is further highlighted. The η_{th} of the six-stroke engine is higher for each value of x_r.

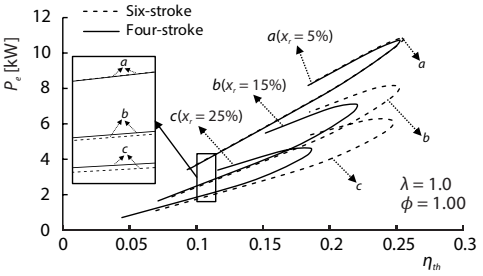

Figure 9. Variations of effective power, P_e, effective thermal efficiency, η_e, against to residual gas fraction, x_r, at fixed stroke ratio, λ, and equivalence ratio, ϕ

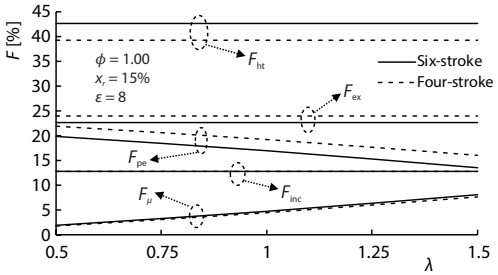

Figure 10. Variations of performance fractions, F, stroke ratio, λ, at fixed equivalence ratio, ϕ, residual gas fraction, x_r, and compression ratio, ε

The effect of λ on performance fractions with ϕ, x_r, and ε fixed is shown in fig. 10. Accordingly, F_{inc}, F_{ht}, and F_{ex} do not have a relationship with λ. As the c_m will change depending on λ, F_μ increases with the increase of λ. There is also a decrease in F_{pe} due to the increase in F_μ. The λ appears to have a considerable effect on F_{pe}. However, in each case, F_{pe} of the six-stroke engine is higher than that of the four-stroke engine.

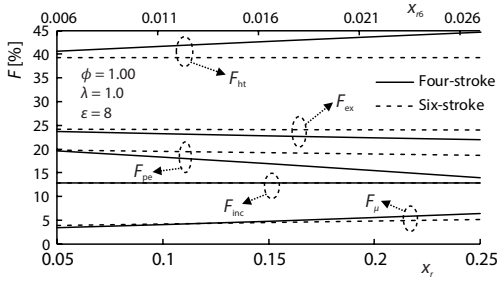

Figure 11. Variations of performance fractions, F, residual gas fraction, x_r, at fixed equivalence ratio, ϕ, stroke ratio, λ, and compression ratio, ε

When x_r increases, F_{ht} and F_μ increase and F_{ex} and F_{pe} decrease, fig. 11. There is no relationship between x_r and F_{inc}. The value of x_{r6} is determined by ε and x_r. Due to the increase in x_r, the F_{ht} change of the six-stroke engine is considerably less than that of the four-stroke engine. This is certainly due to the advantageous situation resulting from the $x_r - x_{r6}$ relationship. This is also the case for F_{pe}. Depending on the x_r, the F_{pe} of the six-stroke engine does not change much, while the F_{pe} of the four-stroke engine is markedly reduced.

The finite time thermodynamics method applied for the four-stroke engine is very similar to the results in the literature. Although the finite time thermodynamics method for the six-stroke engine was applied for the first time, the effects of the design parameters on the engine performance could be successfully examined.

Conclusions

In order to examine the effects of engine design parameters on P_e and η_{th}, a simple simulation model has been presented by using the finite-time thermodynamics method. Parametrical studies were performed for both four- and six-stroke cycle engines. In numerical study, x_r and λ were used as independent variables. Sub-models are carried out for T_1 and η_{com}. Performance loss fractions for engine heat balance are generated for $\dot{m}_f H_u$. Thus, the energy distribution (or also called heat balance) can be examined as dimensionless.

When comparing the four-stroke engine with the six-stroke engine for the same ϕ, P_e of the four-stroke engine and the η_{th} of the six-stroke engine are higher. If η_{th} and P_e are to be high, λ should be preferred low. The six-stroke engine for the same λ can be said to have higher

performance in both Pe_e and η_{th}. The increase in x_r is a disadvantage for both P_e and η_{th}. However, as x_r increases, the performance of the six-stroke engine is quite good compared to the four-stroke engine. The F_{ht}, F_{ex}, and F_{inc} are not related to λ. However, as λ increases, F_μ increases and F_{pe} decreases. The x_r has nothing to do with F_{inc}. However, as x_r increases, F_{ht} and F_μ increase and F_{ex} and P_{pe} decrease. The change of F_{pe} for both engines is not the same, depending on the change of x_r. As x_r increases, F_{pe} curves of the four- and six-stroke engines move away from each other and the six-stroke engine becomes more advantageous than the four-stroke engine.

What is done here is that although it is only a parametric study, the superiority of the novel six-stroke engine compared to the four-stroke engine clearly emerges. The six-stroke engine is cooler and cleaner due to free strokes. In addition, under the same conditions, the six-stroke engine appears to be more advantageous than the four-stroke engine. Highly efficient engines are preferred especially for fuel saving in hybrid electric vehicles. That is, novel six-stroke engines can be used in hybrid electric vehicles.

References

[1] Zhu, S., *et al*., A Review of Water Injection Applied on the Internal Combustion Engine, *Energy Conversion and Management*, *184* (2019), Mar., pp. 139-158
[2] Bae, C., Kim, J., Alternative Fuels for Internal Combustion Engines, *Proceedings of the Combustion Institute*, *36* (2017), 3, pp. 3389-3413
[3] Han, Y., *et al*., Experimental Study of the Effect of Gasoline Components on Fuel Economy, Combustion and Emissions in GDI Engine, *Fuel*, *216* (2018), Mar., pp. 371-380
[4] Noroozian, A., *et al*., Thermodynamic Analysis and Comparison of Performances of Air Standard Atkinson, Otto, and Diesel Cycles with Heat Transfer Considerations, *Heat Transfer-Asian Research*, *46* (2017), 7, pp. 996-1028
[5] Zhao, J., Xu, F., Finite-Time Thermodynamic Modelling and a Comparative Performance Analysis for Irreversible Otto, Miller and Atkinson Cycles, *Entropy*, *20* (2018), 1, 75
[6] Ge, Y., *et al*., Progress in Finite Time Thermodynamic Studies for Internal Combustion Engine Cycles, *Entropy*, *18* (2016), 4, 139
[7] Zhao, J., Research and Application of over-Expansion Cycle (Atkinson and Miller) Engines – A Review, *Applied Energy*, *185* (2017), Part 1, pp. 300-319
[8] Gonca, G., Thermodynamic Analysis and Performance Maps for the Irreversible Dual – Atkinson Cycle Engine (DACE) with Considerations of Temperature-Dependent Specific Heats, Heat Transfer and Friction Losses, *Energy Conversion and Management*, *111* (2016), Mar., pp. 205-216
[9] Constensou, C., Collee, V., The VCR-VVA-High Expansion Ratio, a Very Effective Way to Miller-Atkinson Cycle, SAE Technical Paper, 2016-01-0681, 2016
[10] Peden, M., *et al*., Comparison of 1-D Modelling Approaches for Wankel Engine Performance Simulation and Initial Study of the Direct Injection Limitations, SAE Technical Paper, 2018-01-1452, 2018
[11] Noga, M., Sendyka, B., Determination of the Theorethical and Total Efficiency of the Five-Stroke SI Engine, *International Journal of Automotive Technology*, *15* (2014), 7, pp. 1083-1089
[12] Arabaci, E., Icingur, Y., Thermodynamic Investigation of Experimental Performance Parameters of a Water Injection with Exhaust Heat Recovery Six-Stroke Engine, *Journal of the Energy Institute*, *89* (2016), 4, pp. 569-577
[13] Chen, H., *et al*., A New Six Stroke Single Cylinder Diesel Engine Referring Rankine Cycle, *Energy*, *87* (2015), July, pp. 336-342
[14] Arabaci, E., *et al*., Experimental Investigation of the Effects of Direct Water Injection Parameters on Engine Performance in a Six-Stroke Engine, Energy Conversion and Management, *98* (2015), July, pp. 89-97
[15] Arabacı, E., A Novel Extended Expansion Engine Mechanism, *International Journal of Automotive Science and Technology*, *2* (2018), 2, pp. 16-23
[16] Conklin, J. C., Szybist, J. P., A Highly Efficient Six-Stroke Internal Combustion Engine Cycle with Water Injection for in-Cylinder Exhaust Heat Recovery, *Energy*, *35* (2010), 4, pp. 1658-1664
[17] Gupta, K., *et al*., Design and Experimental Investigations on Six-Stroke SI Engine Using Acetylene with Water Injection, *Environmental Science and Pollution Research*, *25* (2018), June, 23033-23044

[18] Rajput, O., *et al*., Numerical Study on Combustion Characteristics of Six-Stroke-Cycle Gasoline Compression Ignition Engine with Continuously Variable Valve duration Valve Technology, *International Journal of Engine Research*, *22* (2019), 1, pp. 165-183
[19] Vinoth K. I., Pinky, D., Investigation of the Effects of Exhaust and Power Loss in Dual-Fuel Six-Stroke Engine with EGR Technology, *International Journal of Ambient Energy*, *41* (2018), 11, pp. 1270-1275
[20] Kelem, H., Kelem, E.,. U. S., Patent No. 7726268, Washington, DC: U. S. Patent and Trademark Office, 2010
[21] Andresen, B., *et al*., Thermodynamics for Processes in Finite Time, *Accounts of Chemical Research*, *17* (1984), 8, pp. 266-271
[22] Ebrahimi, R., Effect of Volume Ratio of Heat Rejection Process on Performance of an Atkinson Cycle, *Acta Physica Polonica A*, *133* (2018), 1, pp. 201-205
[23] Ebrahimi, R,. Performance Analysis of an Irreversible Miller Cycle with Considerations of Relative Air-Fuel Ratio and Stroke Length, *Applied Mathematical Modelling*, *36* (2012), 9, pp. 4073-4079
[24] Dobrucali, E., The Effects of the Engine Design and Running Parameters on the Performance of a Otto–Miller Cycle Engine, *Energy*, *103* (2016), May, pp. 119-126
[25] Gonca, G., et al., Performance Maps for an Air-Standard Irreversible Dual-Miller Cycle (DMC) with Late Inlet Valve Closing (LIVC) Version, *Energy*, *54* (2013), June, pp. 285-290
[26] Ebrahimi, R., Effects of Mean Piston Speed, Equivalence Ratio and Cylinder Wall Temperature on Performance of an Atkinson Engine, *Mathematical and Computer Modelling*, *53* (2011), 5-6, pp. 1289-1297
[27] Ebrahimi, R., Dehkordi, N. S., Effects of Design and Operating Parameters on Entropy Generation of a Dual Cycle, Journal of Thermal Analysis and Calorimetry, *133* (2018), 3, pp. 1609-1616
[28] Ozdemir, A. O., *et al*., Effect of Mean Piston Speed and Residual Gas Fraction on Performance of a Four-stroke Irreversible Otto Cycle Engine, *Scientific Journal of Mehmet Akif Ersoy University*, *1* (2018), 1, pp. 6-12
[29] Wu, Z., *et al*., Thermodynamic Optimization for an Air-Standard Irreversible Dual-Miller Cycle with Linearly Variable Specific Heat Ratio of Working Fluid, *International Journal of Heat and Mass Transfer*, *124* (2018), Sept., pp. 46-57
[30] Ge, Y., *et al*., Exergy-Based Ecological Performance of an Irreversible Otto Cycle with Temperature-Linear-Relation Variable Specific Heat of Working Fluid, *The European Physical Journal Plus*, *132* (2017), 5, 209
[31] Ge, Y., *et al*., Effects of Heat Transfer and Friction on the Performance of an Irreversible Air-Standard Miller Cycle, *International Communications in Heat and Mass Transfer*, *32* (2005), 8, pp. 1045-1056
[32] Gonca, G., Performance Analysis of an Atkinson Cycle Engine under Effective Power and Effective Power Density Conditions, *Acta Physica Polonica A*, *132* (2017), 4, pp. 1306-1313
[33] Ebrahimi, R., Thermodynamic Modelling of an Atkinson Cycle with Respect to Relative Air-Fuel Ratio, Fuel Mass Flow Rate and Residual Gases, *Acta Physica Polonica A*, *124* (2013), 1, pp. 29-34
[34] Arabaci, E., A Simple Approach for Comparing Performance of Gasoline General-Purpose Engines at Maximum Power (in Turkish), *European Journal of Science and Technology*, (2019), 15, pp. 269-279
[35] Gonca, G., Hocaoglu, M. F., Performance Analysis and Simulation of a Diesel-Miller Cycle (DiMC) Engine, *Arabian Journal for Science and Engineering*, *44* (2019), Feb., pp. 5811-5824
[36] Ge, Y., *et al*., Effect of Specific Heat Variations on Irreversible Otto Cycle Performance, *International Journal of Heat and Mass Transfer*, *122* (2019), July, pp. 403-409

Paper submitted: September 26, 2019
Paper revised: January 28, 2020
Paper accepted: March 10, 2020